European Journal of Pharmacology 667 (2011) 91–99

Contents lists available at ScienceDirect

European Journal of Pharmacology

journal homepage: www.elsevier.com/locate/ejphar

Molecular and Cellular Pharmacology

ErbB protein modifications are secondary to severe cell membrane alterations induced by elisidepsin treatment

Tímea Váradi [a], Janos Roszik [a], Duarte Lisboa [a], György Vereb [a], José Manuel Molina-Guijarro [b], Carlos M. Galmarini [b], János Szöllősi [a,c], Peter Nagy [a,*]

[a] Department of Biophysics and Cell Biology, University of Debrecen, Nagyerdei krt. 98, H-4012 Debrecen, Hungary
[b] Cell Biology Department, PharmaMar, Avda de los Reyes 1, Pol. Ind. La Mina, 28770 Colmenar Viejo (Madrid), Spain
[c] Cell Biology and Signaling Research Group of the Hungarian Academy of Sciences, University of Debrecen, Nagyerdei krt. 98, H-4012 Debrecen, Hungary

ARTICLE INFO

Article history:
Received 20 October 2010
Received in revised form 7 May 2011
Accepted 22 May 2011
Available online 2 June 2011

Keywords:
Elisidepsin
ErbB proteins
Liquid ordered domain
FRET

ABSTRACT

Elisidepsin is a marine-derived anti-tumor agent with unique mechanism of action. It has been suggested to induce necrosis associated with severe membrane damage. Since indirect evidence points to the involvement of ErbB receptor tyrosine kinases and lipid rafts in the mechanism of action of elisidepsin, we investigated the effect of the drug on the distribution of ErbB proteins and systematically compared the elisidepsin sensitivity of cell lines overexpressing ErbB receptors. Stable expression of a single member of the ErbB family (ErbB1-3) or co-transfection of ErbB2 and ErbB3 did not modify the elisidepsin sensitivity of CHO and A431 cells. However, elisidepsin induced the redistribution of ErbB3 and two GPI-anchored proteins (transfected GPI-anchored eGFP and placental alkaline phosphatase) from the plasma membrane to intracellular vesicles without comparable effects on ErbB1 and ErbB2. Elisidepsin increased the binding of a conformational sensitive anti-ErbB3 antibody without modifying the binding of other ErbB2 or ErbB3 antibodies, and it decreased the homoassociation of both ErbB2 and ErbB3. We also found that elisidepsin decreased the fluorescence anisotropy of a membrane specific fluorescent probe and induced a blue shift in the emission spectrum of Laurdan pointing to significant changes in the order of the plasma membrane possibly associated with the formation of liquid ordered domains. Although the distribution of ErbB proteins is preferentially altered by elisidepsin, our data question their role in determining sensitivity to the drug. We assume that induction of liquid ordered domains is the primary action of elisidepsin leading to all the other observed changes.

1. Introduction

Despite ground-breaking discoveries about the molecular background of malignancy and promising new therapeutic approaches cancer remains the leading cause of death in developed countries (Albreht et al., 2008). In addition to rational drug design screening the rich resources of natural habitats also provides a valuable source for drug discovery and development. Kahalalide F has been isolated from *Elysia rufescens*, an indopacific mollusc acquiring and accumulating it from algae (*Bryopsis pennata*) on which the *Elysia* mollusc feeds (Faircloth and Cuevas, 2006). Due to the scarcity of the natural source elisidepsin (Irvalec; PM02734) with a closely related structure has been synthesized (Provencio et al., 2009) which is currently undergoing phase II clinical investigations (Martin-Algarra et al., 2009).

It has been observed that Kahalalide F induces the disruption of lysosomal membranes (Garcia-Rocha et al., 1996), nuclear fragmentation (Suarez et al., 2003) and necrotic cell death (Janmaat et al., 2005; Molina-Guijarro et al., 2009; Suarez et al., 2003). It was also suggested that Kahalalide F and elisidepsin act by inhibiting Akt activity (Janmaat et al., 2005; Ling et al., 2009). A recent paper about elisidepsin reported that *S. cerevisiae* lines mutated in genes involved in the regulation of vesicular trafficking were the most sensitive to the compound (Herrero et al., 2008). RNA interference-mediated knockdown of fatty acid 2-hydroxylase (FA2H) expression increased resistance to elisidepsin suggesting that the enzyme plays a role in the mechanism of action of the drug (Herrero et al., 2008). Fatty acid 2-hydroxylation has been implicated in hydrogen bond formation and stabilization of lipid rafts (Brown and London, 1998).

The ErbB family of receptor tyrosine kinases comprises four members (ErbB1–4) whose ligand-induced or overexpression-driven activation involves the formation of an extensive network of dimers and larger clusters (Citri and Yarden, 2006; Nagy et al., 1999; Szabó et al., 2008). They play a key role in the initiation and progression of several human cancers (Holbro et al., 2003) and are the targets of receptor-oriented therapies (Di Cosimo and Baselga, 2008). It has previously been hypothesized that ErbB protein expression determines Kahalalide F and elisidepsin sensitivity. Some authors pointed

* Corresponding author. Tel.: +36 52 412623; fax: +36 52 532201.
E-mail address: nagyp@med.unideb.hu (P. Nagy).

0014-2999/$ – see front matter © 2011 Elsevier B.V. All rights reserved.
doi:10.1016/j.ejphar.2011.05.064

to ErbB3 as an exclusive factor in determining Kahalalide F sensitivity (Janmaat et al., 2005), while others claimed to have found a correlation between elisidepsin sensitivity and the expression levels of ErbB1, ErbB2 and ErbB3 (Ling et al., 2009). According to these data ErbB3 was efficiently dephosphorylated and degraded by elisidepsin (Ling et al., 2009).

To investigate whether ErbB proteins play a role in determining elisidepsin sensitivity, we analyzed the importance of ErbB1–3 in elisidepsin-induced responses. Here we show that although elisidepsin indirectly affects the association and distribution of ErbB2 and ErbB3, their expression is insufficient to increase the sensitivity of CHO and A431 cell lines to the drug. On the other hand, elisidepsin induced significant alterations in the order of the plasma membrane. We assume that these alterations are the primary actions of elisidepsin which can potentially lead to all the other observed changes including the redistribution of ErbB and GPI-anchored proteins.

2. Materials and methods

2.1. Cells and plasmids

SKBR-3, MCF-7, CHO and A431 cells were obtained from the American Type Culture Collection (ATCC, Manassas, VA) and grown according to their specifications. The CHO-ErbB2-3 cell line stably expressing both ErbB2 and ErbB3 was generated by successive transfections of ErbB2 and ErbB3 into CHO cells using Lipofectamine 2000 (Invitrogen, Carlsbad, CA). The ErbB2–pcDNA3 plasmid obtained from Yosef Yarden (The Weizmann Institute of Science, Rehovot, Israel) was transfected into CHO cells and transfected cells were selected with 1 mg/ml G418. Cells stably expressing ErbB2 in their membrane isolated by flow cytometric sorting of cells showing positive staining with trastuzumab were transfected with ErbB3–pcDNA6. The ErbB3–pcDNA6 plasmid was generated from the YFPN1-ErbB3 plasmid obtained from József Tőzsér (Department of Biochemistry and Molecular Biology, University of Debrecen, Hungary). Briefly, the ErbB3 sequence was amplified by PCR using YFPN1-ErbB3 as the template. The two PCR primers contained restriction sites for KpnI and NotI. The amplified ErbB3 sequence was ligated into a pcDNA6 plasmid (Invitrogen) linearized by KpnI and NotI restriction enzymes. Cells stably transfected with ErbB3–pcDNA6 were selected with 30 μg/ml blasticidin, and were further enriched by flow cytometric sorting of cells showing positive staining with H3.90.6. CHO-ErbB2 and CHO-ErbB2–3 cells were found to express ~2×10^5 ErbB2 and the double-transfected cell line expressed ~10^5 ErbB3 proteins according to flow cytometric characterization by Qifikit (Dako, Glostrup, Denmark). Untransfected CHO cells do not express ErbB1 or ErbB3, but display a very low endogenous expression of ErbB2 undetectable by flow cytometry and Western blotting (Tzahar et al., 1996; Zurita et al., 2004). A431-erbB1-eGFP, A431-erbB2-mYFP and A431-erbB3-citrine cell lines, stably expressing ErbB1-eGFP (ErbB1 fused to enhanced GFP), ErbB2-mYFP (ErbB2 fused to monomeric YFP) and ErbB3-citrine, respectively, were kindly provided by Donna Arndt-Jovin (Max Planck Institute for Biophysical Chemistry, Göttingen, Germany) and have been described elsewhere (Lidke et al., 2004). The ErbB expression profile of the cell lines used in the experiments is summarized in supplementary Table 1. For microscopic experiments cells were cultured in chambered 8-well cover slips (Nalge Nunc International, Rochester, NY). For flow cytometry cells were harvested by trypsinization.

2.2. RNA interference

Cells were transfected with validated "MISSION shRNA" plasmid coding a short hairpin RNA (shRNA) against ErbB3 (TRCN0000009835, NM_001982.x-4705s1c1; sequence: CCGGAGGTTAGGAGTAGATATTGACTCGAGTCAATATCTACTCCTAACCTCTTTTTG; Sigma-Aldrich, St. Louis, MO). Transfection was carried out with the Nucleofector device of Lonza (Cologne, Germany) using solution T and program X-001 for A431 cells and solution C and program E-009 for SKBR-3 cells. Cells were seeded in 96-well plates after transfection and allowed to express shRNA for 60 h followed by a 3-day treatment with elisidepsin.

2.3. Antibodies and chemicals

The anti-ErbB2 antibody, trastuzumab (Herceptin®) was purchased from Roche (Budapest, Hungary). Anti-ErbB3 antibodies H3.90.6, H3.90.12 and H3.105.5 were obtained from LabVision/Thermo Fisher Scientific (Fremont, CA). Monoclonal anti-PLAP (placental alkaline phosphatase, A2951) and anti-actin (A4700) antibodies were purchased from Sigma-Aldrich. The conjugation of primary antibodies with AlexaFluor488, AlexaFluor546 and AlexaFluor647 (Molecular Probes/Invitrogen, Eugene, OR) dyes was carried out according to the manufacturer's specifications. Alexa647-conjugated $F(ab')_2$ fragment of goat anti-mouse IgG was purchased from Molecular Probes/Invitrogen (Eugene, OR). Heregulin-β1 was obtained from R&D Systems (Minneapolis, MN). 4′-(trimethylammonio)-diphenylhexatriene (TMA-DPH) and Laurdan (6-dodecanoyl-N,N-dimethyl-2-naphthylamine) were purchased from Sigma-Aldrich. TMA-DPH and Laurdan were dissolved in tetrahydrofuran and dimethyl sulfoxide, respectively. Elisidepsin was manufactured by PharmaMar (Madrid, Spain) and dissolved in dimethyl sulfoxide at a concentration of 1 mg/ml.

2.4. Western blotting

Cells were lysed in Ripa buffer supplemented with protease and phosphatase inhibitor cocktails (Roche). Protein extracts were resolved in denaturing polyacrylamide gels and electroblotted to PVDF membranes. Expressions of ErbB2 and ErbB3 receptors were detected using mAb#2248 and mAb#4754, respectively (Cell Signaling Technology, Danvers, MA).

2.5. Measurement of cell viability

The short-term cytotoxic effect of elisidepsin was tested by microfluorometric propidium iodide uptake assay. Cells were seeded at high density in black, clear bottom 96-well microtiter plates and allowed to grow to confluency. Fresh culture medium (supplemented with 25 mM HEPES, pH 7.4, and 50 μg/ml propidium iodide) in the absence or presence of different concentrations of elisidepsin was added in quadruplicates and the uptake of propidium iodide was quantified by plate fluorimetry at excitation and emission wavelengths of 531 and 632 nm, respectively, at 37 °C using a Victor3 Multilabel Counter (Perkin Elmer, Waltham, MA). The long-term effect of elisidepsin on cell viability was assayed by measuring the oxidation of a water-soluble tetrazolium salt by mitochondrial dehydrogenases using the cell proliferation reagent WST-1 (Roche Diagnostics GmbH, Mannheim, Germany). Cells (7×10^3) were plated into single wells of 96-well plates 24 h before the experiment. Cells were treated with a dilution series of elisidepsin for 2 h in triplicate followed by incubation for 72 h in cell culture medium in a CO_2 incubator at 37 °C. The absorbance of the WST-1 reagent was measured by an ELISA reader at 450 nm and 620 nm. The IC50 value, the concentration leading to the death of 50% of the cells, was determined by fitting the following equation to the normalized absorbance data using the 'fit' command of Matlab (Mathworks Inc., Natick, MA):

$$A_{min} + \frac{A_{max} - A_{min}}{1 + 10^{n\,(\log(c) - \log(IC50))}} \quad (1)$$

where A_{min} and A_{max} are the lowest and highest absorbance values, respectively, n is the Hill coefficient, c is the concentration of elisidepsin and log is logarithm with base 10.

2.6. Statistical analysis of cell viability

One-way analysis of variance (ANOVA) was used to compare the IC50 values and the propidium iodide fluorescence intensities (at 30 and 60 min) of the different cell lines using SigmaStat (Systat Inc., San Jose, CA).

2.7. Fluorescence resonance energy transfer (FRET)

FRET was measured with a FacsArray flow cytometer (Becton Dickinson, Franklin Lakes, NJ). Antibodies labeled with AlexaFluor546 and AlexaFluor647 were used as donor and acceptor, respectively. The donor, FRET and acceptor fluorescence intensities were measured in the Yellow, Far Red and Red channels, respectively. The Yellow and Far Red intensities were excited with a 532 nm solid state laser and detected using a 585/42 nm bandpass and a 685 nm longpass filter, respectively. The Red intensity was excited at 635 nm using a diode laser and measured using a 661/16 nm bandpass filter. The necessary controls, calibration samples and evaluation principles have been described elsewhere (Nagy et al., 2006). The FRET efficiency was calculated on a cell-by-cell basis using the ReFlex software (www.freewebs.com/cytoflex) (Szentesi et al., 2004).

2.8. Confocal microscopy

A Zeiss LSM510 confocal laser scanning microscope (Carl Zeiss AG, Jena, Germany) was used to image fluorescently stained cells. AlexaFluor488 was excited with the 488 nm line of an argon ion laser and its fluorescence was detected above 505 nm. The emission of eGFP excited at 488 nm was recorded with a 505 long-pass filter. mYFP and citrine were excited at 514 nm and detected above 530 nm. Confocal stacks were acquired with the pinhole size adjusted to 1 Airy unit and image distances of 0.5 μm along the Z axis using a 63× (NA = 1.4) oil immersion objective. Image analysis and the preparation of orthogonal projections were carried out with a custom-written Matlab (Mathworks Inc., Natick, MA) program incorporating DipImage commands (Delft University of Technology, Delft, The Netherlands).

2.9. Measurement of fluorescence anisotropy and generalized polarization

Trypsinized cells were resuspended in Hank's buffer at a concentration of 10^7/ml and labeled with 2 μM TMA-DPH or 2.5 μM Laurdan at room temperature for 20 min. After TMA-DPH labeling cells were diluted in Hank's buffer without washing to a concentration of 10^6/ml for fluorescence anisotropy measurements, whereas Laurdan-labeled cells were washed once and resuspended at a concentration of 10^6/ml in Hank's buffer. Fluorescence measurements were carried out with a Fluorolog-3 spectrofluorimeter (Horiba Jobin Yvon, Edison, NJ). The temperature of the cuvette holder was adjusted to 37 °C by a circulating water bath. TMA-DPH was excited at 352 nm and its emission was measured at 430 nm. The fluorescence anisotropy (r) of TMA-DPH was measured in the L-format according to the following formula (Kuhry et al., 1983; Lakowicz, 2006):

$$r = \frac{I_{vv} - GI_{vh}}{I_{vv} + 2GI_{vh}} \quad (2)$$

where I_{vv} and I_{vh} are the vertical and horizontal components, respectively, of the fluorescence excited by vertically polarized light, and G is a correction factor characterizing the different sensitivity of the detection system for vertically and horizontally polarized light:

$$G = \frac{I_{hv}}{I_{hh}} \quad (3)$$

where I_{hv} and I_{hh} are the vertical and horizontal components, respectively, of the fluorescence excited by horizontally polarized light. Laurdan was excited at 350 nm and its emission was detected in the blue range of its emission spectrum at 435 nm (I_{blue}) and at the red edge at 500 nm (I_{red}). Generalized polarization (GP) of Laurdan fluorescence was calculated according to the following formula (Harris et al., 2002; Parasassi et al., 1991; Sanchez et al., 2007):

$$GP = \frac{I_{blue} - I_{red}}{I_{blue} + I_{red}}. \quad (4)$$

3. Results

3.1. Expression of ErbB1–3 does not alter the sensitivity of CHO and A431 cells to elisidepsin

In order to investigate the role of ErbB2 and ErbB3 in elisidepsin sensitivity we have established two CHO-derived cell lines stably expressing ErbB2 (CHO-ErbB2) or ErbB2 and ErbB3 (CHO-ErbB2–3). Western blotting confirmed that the cell lines expressed the transfected proteins (Fig. 1A). Further flow cytometric analysis demonstrated that CHO cells do not express any of the ErbB proteins at levels detectable by this technique (data not shown) in agreement with previous reports (Tzahar et al., 1996; Zurita et al., 2004). CHO-ErbB2-3 cells were found to express ~2×10^5 ErbB2 and ~10^5 ErbB3. The expression levels of ErbB2 in CHO-ErbB2 and CHO-ErbB2–3 were comparable (Supplementary Table 1).

In order to investigate the long-term effect of elisidepsin on viability the parental CHO cells and the two derivative cell lines were treated with different concentrations of elisidepsin for 2 h and the cells were allowed to grow for 3 days in the absence of the drug. The three cell lines were found to be equally sensitive to elisidepsin (IC50 in CHO cells (mean ± standard error of the mean): 10 ± 0.7 μM; IC50 in CHO-ErbB2 cells: 10.5 ± 0.9 μM; IC50 in CHO-ErbB2-3 cells: 10.3 ± 0.8 μM; $p>0.1$ using analysis of variance; Fig. 1B). The effect of elisidepsin on cell survival/proliferation was not significantly affected by increasing the incubation time from 2 h to 3 days (data not shown) implying that the drug exerts its cytotoxic effects very early during drug exposure. In order to analyze the short-term effect of elisidepsin on viability and to investigate the time course of elisidepsin-induced killing we followed the uptake of propidium iodide in the presence of different concentrations of the drug for one hour. Both the extent and kinetics of elisidepsin-induced membrane permeabilization were comparable in the three cell lines since comparison of fluorescence intensities using analysis of variance did not provide evidence for significant differences among them ($p>0.1$, Fig. 1C).

In order to confirm the lack of effect of ErbB protein expression on elisidepsin sensitivity in another cell line we checked the short- and long-term effects of the drug on A431 cells and its subclones stably transfected with ErbB1-eGFP, ErbB2-mYFP or ErbB3-citrine (A4erbB1, A4erbB2 and A4erbB3 cells, respectively). The ErbB expression profile of these cell lines is summarized in supplementary Table 1. Similar to CHO cells introduction of ErbB proteins (ErbB1–3) into A431 did not change the long-term sensitivity of cells to elisidepsin (IC50 in A431: 8.2 ± 0.8 μM; IC50 in A4erbB1: 9.4 ± 0.5 μM; IC50 in A4erbB2: 9.9 ± 1.0 μM; IC50 in A4erbB3: 9.9 ± 0.9 μM; $p>0.1$ using analysis of variance; Fig. 2A). The short-term effectiveness of elisidepsin was not altered by overexpression of any of the ErbB proteins either ($p>0.1$ using analysis of variance; Fig. 2B, Fig. S1). We concluded that the elisidepsin-induced cytotoxic effect is a rapid event and the expressions of ErbB1, ErbB2 and ErbB3 do not influence the sensitivity of cells to the drug.

The lack of any effect of ErbB3 overexpression in cells showing no or weak expression of the protein on elisidepsin sensitivity strongly implies that ErbB3 does not influence elisidepsin sensitivity. However, several previous reports presented evidence for the role of ErbB3 in the mechanism of action of the drug. Therefore, we

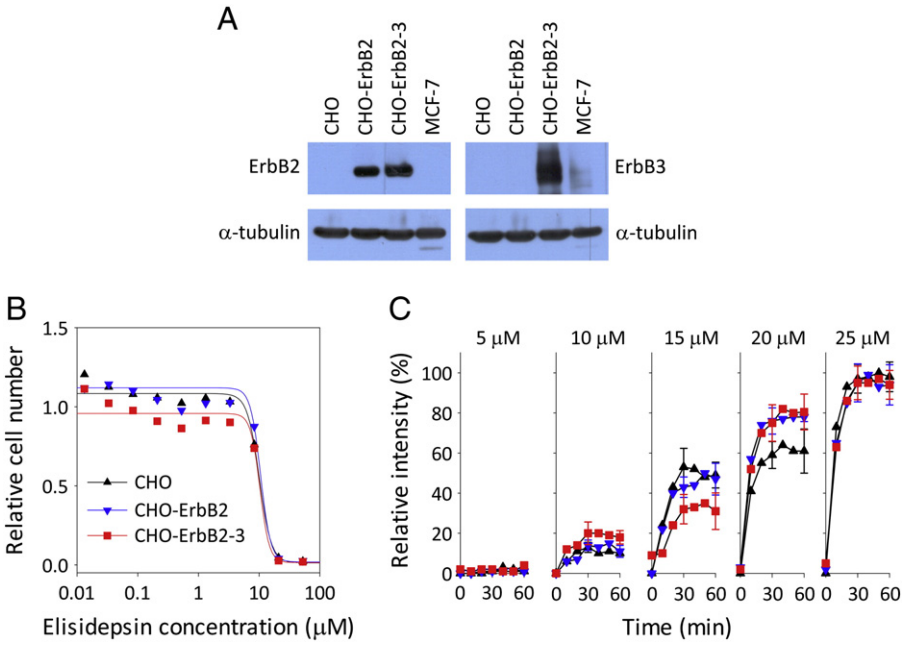

Fig. 1. Expression of ErbB2 and ErbB3 proteins in CHO cells does not increase their sensitivity for elisidepsin. A. Expression of ErbB2 and ErbB3 verified by Western blotting. Whole cell lysates of MCF-7 breast cancer cells, untransfected and transfected CHO cells were separated by SDS-PAGE followed by blotting with an anti-ErbB2 or anti-ErbB3 antibody. Membranes were stripped and reprobed with an anti-α-tubulin antibody. B. Long-term effect of elisidepsin on the viability of wild-type and transfected CHO cells. Untransfected CHO, CHO-ErbB2 and CHO-ErbB2-3 cells were plated in 96-well plates and treated in triplicate with elisidepsin for 2 h. Cells were cultured for another 3 days in the absence of elisidepsin and cell numbers were determined at the end of the experiment using the WST-1 reagent. Counts were normalized to untreated cells and are shown by the symbols as a function of elisidepsin concentration. The lines show the result of fitting according to Eq. 1. C. Short-term effect of elisidepsin on the viability of untransfected and transfected CHO cells. Confluent cultures of CHO, CHO-ErbB2 and CHO-ErbB2-3 cells were treated with the indicated concentrations of elisidepsin for 60 min and the uptake of propidium iodide was followed by microfluorometry during the treatment. Fluorescence intensities were normalized to the maximum measured intensity in the presence of the highest concentration of the drug. The cell lines are marked by the same symbols as in part B. Error bars, shown only at 30 and 60 min for discernibility, indicate the standard error of the mean of four independent measurements. Two ANOVA tests were performed using fluorescence intensities at 30 and 60 min and they did not provide evidence for a significant difference between the cell lines ($p>0.1$).

wanted to confirm our conclusion using RNA interference-mediated knock-down of ErbB3 production. In addition to A431 we have chosen SKBR-3 cells displaying a lower IC50 value for elisidepsin (1.5 ± 0.2 μM, data not shown). Two days after transfection with an ErbB3 shRNA plasmid the expression level of ErbB3 was reduced by ~85% corresponding to an expression level of ~500 and ~2500 in A431 and SKBR-3 cells, respectively (Fig. S2). The IC50 of the transfected cells did not significantly differ from control cells (IC50 in mock-transfected SKBR-3: 2.64 ± 0.8 μM; IC50 in ErbB3 shRNA-transfected SKBR-3: 2.82 ± 1.1 μM; IC50 in mock-transfected A431: 9.48 ± 1.2 μM; IC50 in ErbB3 shRNA-transfected A431: 8.55 ± 1.4 μM) corroborating that elisidepsin responsiveness does not depend on ErbB3 expression (Fig. 3).

3.2. Elisidepsin specifically increases the binding of a conformation-sensitive anti-ErbB3 antibody

Our results presented in the previous section refute evidence for the role of ErbB proteins in elisidepsin sensitivity. However, it is still possible that the reported effects of elisidepsin on ErbB proteins are not artifacts, but rather indirect effects of the drug. Therefore, we performed several experiments to reveal if elisidepsin exerts any

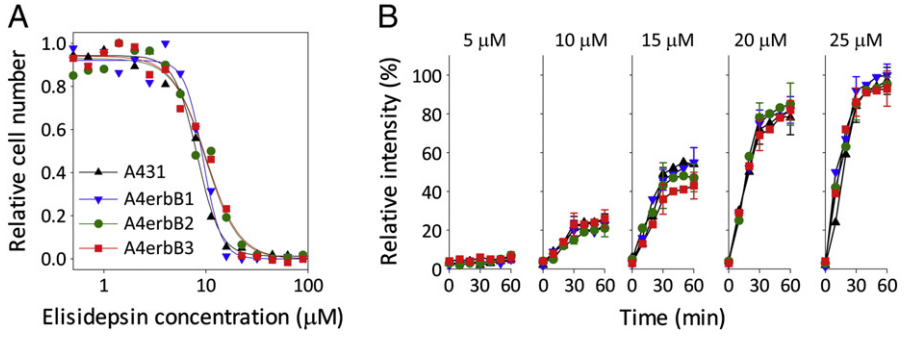

Fig. 2. Transfection of A431 cells with ErbB proteins does not influence their sensitivity for elisidepsin. A. Long-term effect of elisidepsin on the viability of wild-type and transfected A431 cells. Untransfected, ErbB1-eGFP- (A4erbB1), ErbB2-mYFP- (A4erbB2) and ErbB3-citrine-transfected (A4erbB3) A431 cells were plated in 96-well plates, treated with different concentrations of elisidepsin in triplicate for 2 h followed by culturing in the absence of the drug for 3 days. Cell numbers normalized to untreated cells are plotted as a function of elisidepsin concentration. The symbols and the lines show the measured data points and the result of fitting according to Eq. 1, respectively. B. Short-term effect of elisidepsin on the viability of untransfected and transfected A431 cells. Confluent cultures of A431, A4erbB1, A4erbB2 and A4erbB3 cells were treated with the indicated concentrations of elisidepsin for 60 min and the uptake of propidium iodide was followed by microfluorometry during the treatment. Fluorescence intensities were normalized to the maximum measured intensity in the presence of the highest concentration of the drug. The cell lines are marked by the same symbols as in part A. Error bars, shown only at 30 and 60 min to avoid clutter, indicate the standard error of the mean of four independent measurements. Statistical analysis was carried out as described in the legend to Fig. 1.

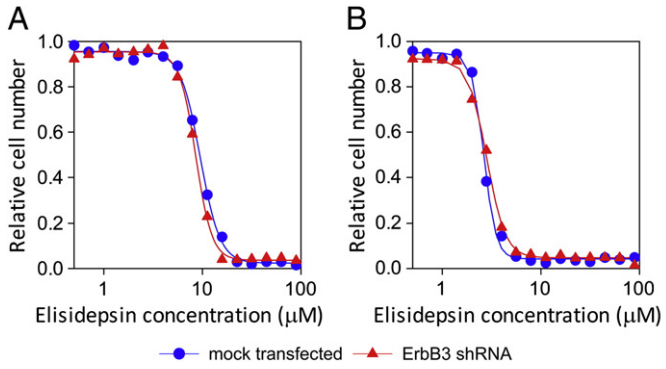

Fig. 3. RNA interference-mediated suppression of ErbB3 expression does not modify elisidepsin sensitivity. A431 (A) and SKBR-3 (B) cells were transfected with a plasmid expressing a shRNA against ErbB3. Control, mock transfected cells were treated identically in the absence of the plasmid. Sixty hours after transfection cells were treated with the indicated concentrations of elisidepsin for 2 h in triplicate followed by culturing in the absence of the drug for another 3 days.

influence on ErbB proteins. First, we tested whether the binding of antibodies against ErbB2 or ErbB3 is altered by treatment of cells with 10 μM elisidepsin. Elisidepsin-treated and control CHO-ErbB2-3 cells were fixed, permeabilized and stained with fluorescent antibodies followed by flow cytometric analysis. Since the staining was carried out with permeabilized cells, the measured fluorescence intensities reflected the total amount of the antigen in single cells. Although elisidepsin did not alter the binding of two anti-ErbB2 (trastuzumab, pertuzumab) and two anti-ErbB3 antibodies (H3.90.6, H3.90.12), it significantly enhanced the amount or accessibility of the epitope for another antibody against ErbB3, H3.105.5 (Fig. 4). In the absence of elisidepsin the binding of the H3.105.5 antibody to CHO-ErbB2-3 cells was negligible which was significantly increased by elisidepsin. The increased binding of H3.105.5 was abolished by heregulin, the ligand of ErbB3 which is known to compete with the H3.105.5 antibody. Our results indicate that elisidepsin may induce a conformational change of ErbB3 leading to an altered accessibility of the epitope for the H3.105.5 antibody.

3.3. Elisidepsin decreases the homoassociation of ErbB2 and ErbB3

The direct or indirect involvement of a protein in the action of a drug is often reflected in the altered association state of the protein. Since the previous results imply that ErbB3 is affected by elisidepsin, we tested whether the homo- and heteroassociations of ErbB2 and ErbB3 are altered by elisidepsin treatment. Flow cytometric FRET measurements revealed that while the homoassociations of both ErbB2 and ErbB3 were significantly decreased by elisidepsin, their heteroassociation did not change (Fig. 5). The FRET efficiencies for the heteroassociation of ErbB2 and ErbB3 were markedly different when the donor and acceptor antibodies were swapped. This finding is in accordance with the dependence of FRET efficiency on the quantity of the acceptor (Kenworthy and Edidin, 1998). The elisidepsin-induced effect on the homoassociations of ErbB2 and ErbB3 were dose-dependent and the drug concentrations required for the cytotoxic effect and the impact on the homoassociations were comparable. These findings imply that the observed changes in the homoassociations of ErbB2 and ErbB3 are indirectly linked to the mechanism of action of elisidepsin although neither ErbB2 nor ErbB3 is necessary for elisidepsin sensitivity.

3.4. Elisidepsin induces the redistribution of ErbB3 and GPI-anchored proteins into the intracellular space

FRET measurements are sensitive for the interactions of proteins on the molecular scale, but the distribution of molecules and their clustering on the micrometer scale are not revealed. In order to show the effect of elisidepsin on this latter dimension of associations control and elisidepsin-treated CHO-ErbB2-3 cells were fixed, permeabilized and stained with fluorescent antibodies against ErbB2 and ErbB3. Confocal microscopy convincingly showed that elisidepsin did not change the distribution of ErbB2, while that of ErbB3 was significantly altered in that the drug induced the redistribution of the protein from the plasma membrane to the intracellular space. Sometimes a distribution pattern typical of nuclear localization was also observed (Fig. 6). In order to corroborate the selective effect of elisidepsin on the distribution of ErbB3 we investigated A431 cells stably transfected with one of ErbB1–3 fused to spectral variants of GFP. While

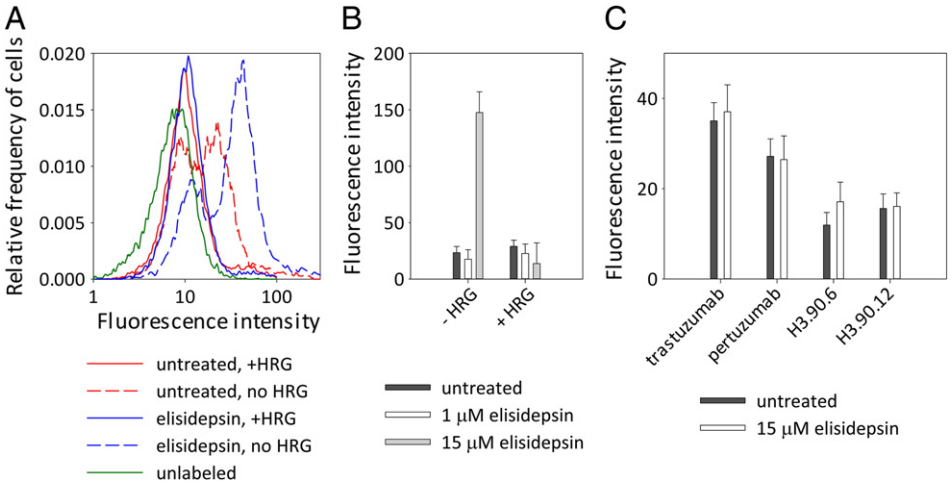

Fig. 4. Elisidepsin-induced changes in the binding of anti-ErbB2 and anti-ErbB3 antibodies. A. Control CHO-ErbB2-3 cells were fixed, permeabilized and labeled by fluorescent anti-ErbB3 antibody H3.105.5 in the absence or presence of heregulin (HRG). Cells treated with 15 μM elisidepsin for 30 min were also labeled by H3.105.5 in the absence or presence of heregulin. The fluorescence histograms of 10,000 labeled cells and that of unlabeled cells recorded by flow cytometry in a typical experiment are plotted in the figure. The means of these measurements are shown in B. B. Fixed and permeabilized control CHO-ErbB2-3 cells and those treated with 1 μM and 15 μM elisidepsin were stained with fluorescent H3.105.5 in the presence (+HRG) and absence (−HRG) of heregulin. Background-corrected mean fluorescence intensities of three independent measurements (±standard error of the mean) are shown in the figure. C. Fixed and permeabilized control (CHO-ErbB2-3) cells and those treated with 15 μM elisidepsin were stained with fluorescent trastuzumab, pertuzumab (both against ErbB2), H3.90.6 or H3.90.12 (both against ErbB3). Background-corrected mean fluorescence intensities of three independent flow cytometric measurements (±standard error of the mean) are plotted in the figure.

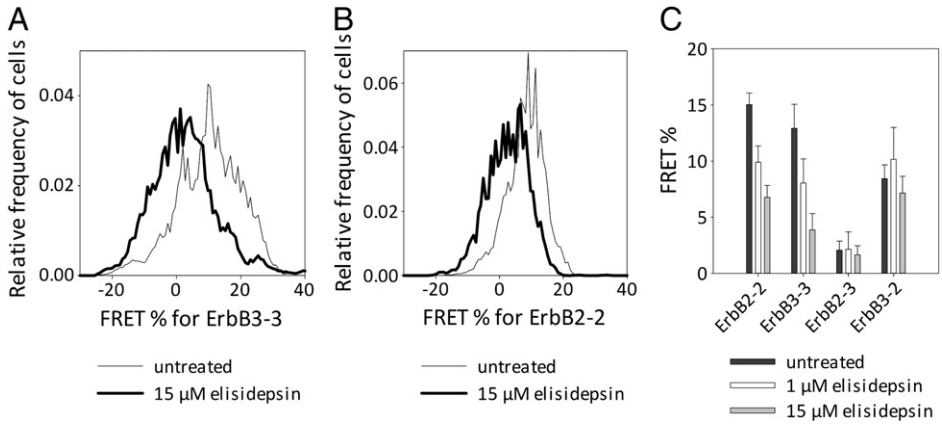

Fig. 5. Elisidepsin-induced changes in the homo- and heteroassociation of ErbB2 and ErbB3. A. CHO-ErbB2-3 cells were treated with 15 μM elisidepsin for 30 min followed by labeling control and the elisidepsin-treated cells with a mixture of donor- and acceptor-conjugated anti-ErbB3 antibodies (H3.90.6). The efficiency of FRET in 10,000 cells was determined by flow cytometry. B. Control CHO-ErbB2-3 cells and those treated with 15 μM elisidepsin for 30 min were labeled with a mixture of donor- and acceptor-tagged anti-ErbB2 antibodies (trastuzumab) and the FRET efficiency of 10,000 cells was determined by flow cytometry. C. Control cells and those treated with 1 μM or 15 μM elisidepsin were analyzed by flow cytometric energy transfer measurements. ErbB2–2 and ErbB3–3 designate the homoassociation of ErbB2 and ErbB3, respectively. ErbB2–3 stands for the heteroassociation of ErbB2 and ErbB3 in the sample in which ErbB2 and ErbB3 were labeled by donor-conjugated and acceptor-conjugated antibodies, respectively. The donor and acceptor fluorophores were reversed in the sample designated by ErbB3–2, i.e. ErbB2 and ErbB3 were labeled by acceptor-conjugated and donor-conjugated antibodies, respectively. The columns and the error bars represent the means and their standard errors, respectively, determined from three independent measurements.

elisidepsin (10 μM) did not affect the typical membrane localization of ErbB1 and ErbB2, ErbB3 accumulated intracellularly upon treatment with the drug displaying a distribution pattern typical of intracellular vesicles (Fig. 7). Since lipid rafts were also implicated in the mechanism of action of elisidepsin (Herrero et al., 2008) and the GPI-anchor is known to localize proteins to lipid rafts (Brown and London, 1998; Sharma et al., 2004), we investigated the effect of the drug (10 μM) on the distribution of GPI–eGFP transiently transfected to A431 cells. GPI-eGFP was present both in the plasma membrane and in intracellular vesicles in untreated cells, but an almost exclusive localization in vesicles was observed after elisidepsin treatment (Fig. 7). In order to exclude the possibility that GPI-anchored eGFP does not represent the native distribution of GPI-anchored proteins we repeated the experiments by immunofluorescent labeling of an endogenous GPI-anchored protein, placental alkaline phosphatase (PLAP), in A431 cells. In untreated cells PLAP exhibited preferential membrane localization which was changed to a pattern characteristic of vesicular or diffuse intracellular distribution (Fig. 8). These results imply that elisidepsin selectively induces the redistribution of GPI-anchored proteins and ErbB3 from the plasma membrane.

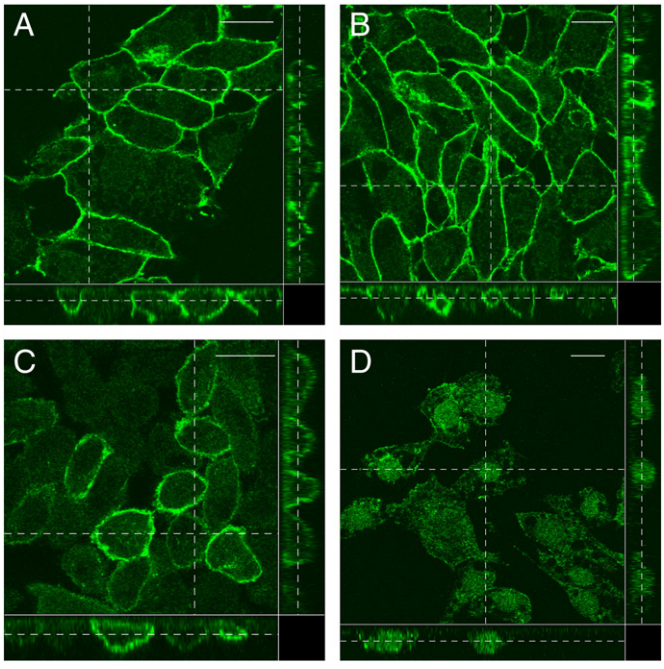

Fig. 6. Elisidepsin induces redistribution of ErbB3 without affecting ErbB2 in CHO cells. A,C: Control (A) CHO-ErbB2-3 cells and those treated with 10 μM elisidepsin for 30 min (C) were fixed, permeabilized and stained with AlexaFluor647-labeled trastuzumab against ErbB2. B,D: Control (B) and elisidepsin-treated (D) CHO-ErbB2-3 cells were fixed, permeabilized and stained with AlexaFluor647-labeled H3.90.6 against ErbB3. Orthogonal sections of confocal microscopy image stacks are shown. Bar = 10 μm.

3.5. Elisidepsin induces abrupt changes in the order of the plasma membrane

The finding that elisidepsin exerts many effects on the interactions and distribution of ErbB proteins is in contrast with the lack of effect of ErbB protein overexpression on elisidepsin sensitivity. We attempted to relieve this apparent contradiction by assuming that all the changes induced by elisidepsin observed by us and others, including the redistribution of membrane proteins and membrane permeabilization, are the consequences of primary membrane effects caused by the drug. Since drugs whose primary target is the plasma membrane have been shown to induce changes in the fluidity or order of the lipid bilayer (Balogh et al., 2005; Engelke et al., 1997; Sear, 2009), we used two fluorescent probes to investigate this aspect of the mechanism of action of elisidepsin. The fluorescence anisotropy of TMA-DPH specifically reports on the microviscosity (fluidity) of the plasma membrane since it cannot cross the cell membrane and enter the membrane of intracellular organelles due to its positive charge (Harris et al., 2002; Kuhry et al., 1983; Matkó and Nagy, 1997). Treatment of A431 cells with 10 μM elisidepsin induced an almost instantaneous decrease in the fluorescence anisotropy of TMA-DPH indicating an increased membrane fluidity followed by a gradual and incomplete return of anisotropy to the initial value in ~20 min (Fig. 9A). The generalized polarization of Laurdan is a sensitive measure of the order of the plasma membrane and of the extent of penetration of water molecules into the plasma membrane (Harris et al., 2002; Parasassi et al., 1991; Sanchez et al., 2007). The generalized polarization of Laurdan was already increased by elisidepsin in one minute, it peaked at ~2 min and gradually and partially declined toward the initial value in ~20 min (Fig. 9B). The increased generalized polarization of Laurdan indicates a higher order of the plasma membrane and a restricted access of water to Laurdan in the plasma membrane.

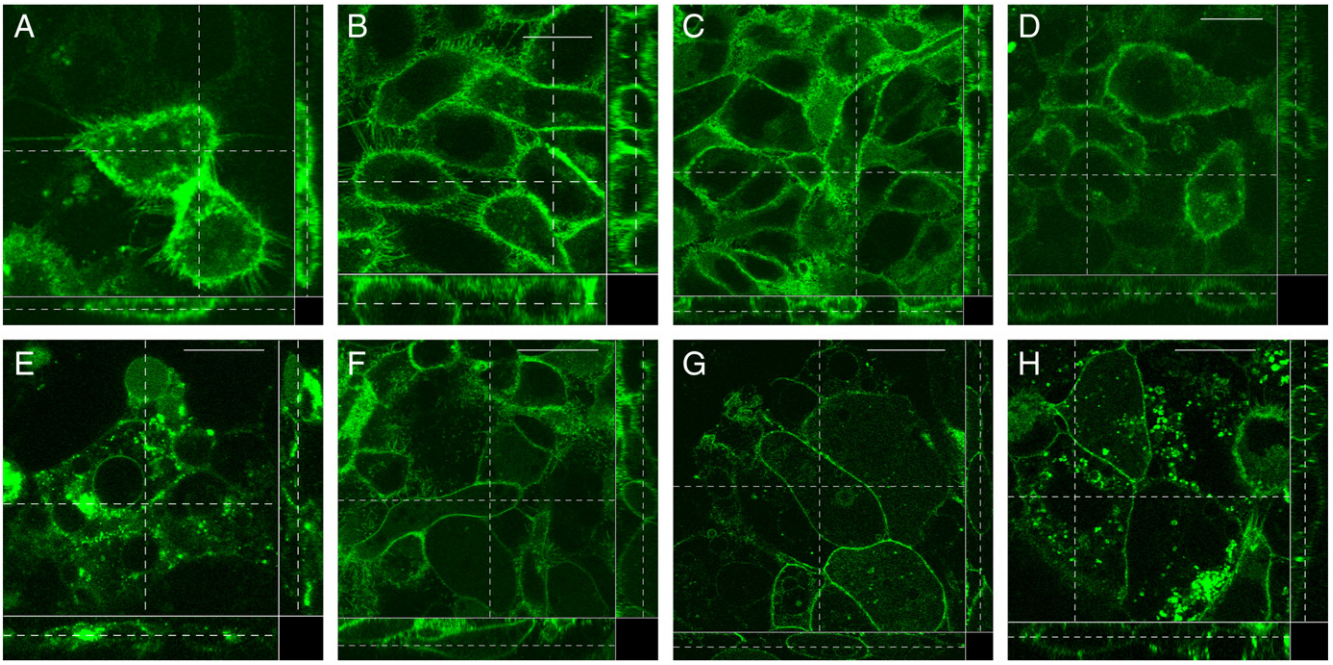

Fig. 7. Elisidepsin preferentially induces internalization of GPI-anchored eGFP and ErbB3-citrine in A431 cells. A431 cells expressing GPI-eGFP, ErbB1-GFP, ErbB2-mYFP or ErbB3-citrine were treated with 10 μM elisidepsin for 30 min and confocal microscopy images of control (top row) and treated cells (bottom row) were acquired. Bar = 10 μm. A,E: Control (A) and elisidepsin-treated (E) A431 cells transiently transfected with GPI-eGFP. B,F: Control (B) and elisidepsin-treated (F) A431 cells stably expressing ErbB1-eGFP (A4erbB1 cells). C,G: Control (C) and elisidepsin-treated (G) A431 cells stably expressing ErbB2-mYFP (A4erbB2 cells). D,H: Control (D) and elisidepsin-treated (H) A431 cells stably expressing ErbB3-citrine (A4erbB3 cells).

Dimethyl sulfoxide, the vehicle of elisidepsin, did not induce any significant change in the anisotropy of TMA-DPH or the generalized polarization of Laurdan.

In order to establish that the observed membrane effects of elisidepsin are not unique to the A431 cell line we repeated the experiments with SKBR-3 cells displaying higher sensitivity to elisidepsin. The overall tendency of the elisidepsin-induced changes in the anisotropy of TMA-DPH and in the generalized polarization of Laurdan in SKBR-3 cells was similar to that observed in A431 cells (Fig. 9C,D). The effect size was slightly bigger in SKBR-3 than in A431 cells and the changes were less transient in the former case. The abrupt and specific changes in the order and fluidity of the lipid bilayer support our assumption that the primary target of elisidepsin is the plasma membrane.

4. Discussion

Here we demonstrate that although elisidepsin induced changes in the homoassociation and cellular distribution of ErbB and GPI-anchored proteins, its cytotoxic effect was independent of the expression of ErbB1–3. On the other hand, elisidepsin was found to induce significant alterations in the order and fluidity of the plasma membrane. All of the observed effects were detected at comparable doses of the drug implying that they are either parts or consequences of its mechanism of action. Previous reports pinpointed ErbB3 (Janmaat et al., 2005) or ErbB1–3 proteins (Ling et al., 2009) as key factors determining Kahalalide F and elisidepsin sensitivity. The fact that the elisidepsin sensitivity of CHO- and A431-derived cell lines did not correlate with their ErbB protein expression levels argues against a decisive role of ErbB receptors in determining elisidepsin responsiveness. In particular, the finding that overexpression of ErbB2 or ErbB2 and ErbB3 in CHO cells (displaying no expression of ErbB1, -3 and -4 and very weak expression of ErbB2) did not alter elisidepsin sensitivity is a strong evidence for the lack of involvement of ErbB2 and ErbB3 in conferring elisidepsin sensitivity. The lack of influence of ErbB3 on elisidepsin responsiveness was also confirmed by showing that RNA interference-mediated knock-down of ErbB3 expression failed to alter the IC50 value for elisidepsin. We excluded the

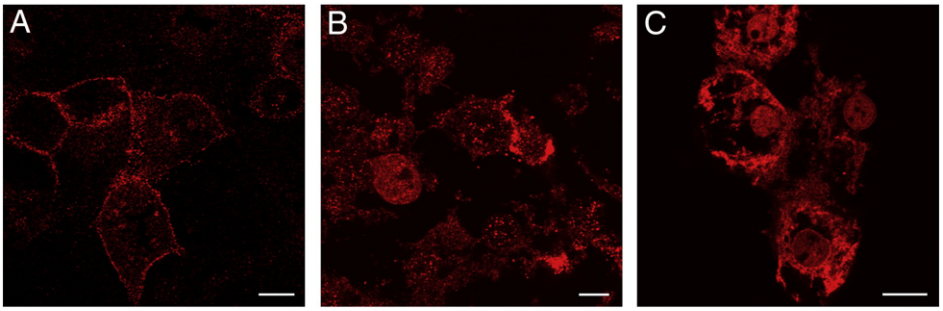

Fig. 8. Distribution of PLAP in control and elisidepsin-treated A431 cells. Control (A) and elisidepsin-treated (10 μM, 30 min; B–C) A431 cells were fixed, permeabilized and labeled with a monoclonal antibody against PLAP. Visualization of the distribution of the protein was achieved by secondary staining with AlexaFluor647-conjugated goat anti-mouse IgG. Bar = 10 μm.

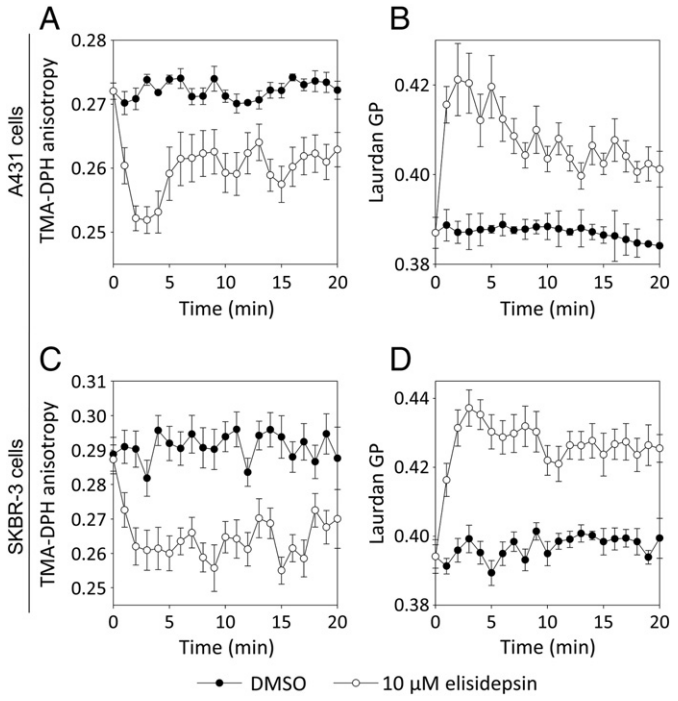

Fig. 9. Elisidepsin-induced changes in the order of the plasma membrane. The fluorescence anisotropy of TMA-DPH (A,C) and the generalized polarization of Laurdan (B,D) were measured in cells treated with 10 μM elisidepsin or with an identical volume of DMSO. The mean ± standard error of three independent measurements is plotted in the top (A,B) and bottom (C,D) figures displaying the results obtained with A431 and SKBR-3 cells, respectively.

possibility that the transfected ErbB proteins were non-functional by showing that EGF and heregulin induced tyrosine phosphorylation of the transfected proteins (data not shown). Consequently, we think that the reported correlations between elisidepsin responsiveness and ErbB receptor expression levels were indirect effects related to drug-induced alterations in the cell membrane.

The IC50 values in the cell lines we tested were somewhat higher than those published earlier ranging between 0.1 and 9 μM (Ling et al., 2009). This difference could be due to different methodologies used in the previous studies compared to ours. In fact elisidepsin was applied for several days (usually 72 h) in previous experiments obtaining lower IC50 values than those determined by us, while we treated cells for a shorter period of time. It is worth noting that the half-life of Kahalalide F is ~30 min in patients, so the brief in vitro treatment with elisidepsin is likely to mimic the in vivo situation (Martin-Algarra et al., 2009).

Elisidepsin induces characteristic changes in the order of the plasma membrane almost immediately after administration while changes in the association and distribution of membrane proteins (GPI-anchored and ErbB proteins) take place after a longer period of time. Therefore, we assume that the alterations in the distribution and association of ErbB and GPI-anchored proteins are the consequences of the elisidepsin-induced change in the structure of the membrane. Flow cytometric FRET investigations revealed that elisidepsin induces a decrease in the homoassociations of ErbB2 and ErbB3 without measurable changes in their heteroassociations. Both ErbB2 and ErbB3 have been found to form large-scale associations involving tens of proteins in quiescent cells (Landgraf and Eisenberg, 2000; Szabó et al., 2008). We assume that large protein clusters are preferentially disrupted as a result of the membrane alterations induced by elisidepsin since membrane-mediated interactions are thought to play a fundamental role in driving the formation of large protein aggregates (Kusumi et al., 2010). On the other hand, direct protein–protein interactions, which are not expected to be subverted by the membrane damage caused by elisidepsin, are responsible for the creation of small protein clusters. Although conventional flow cytometric hetero-FRET measurements are not exquisitely suited for the determination of cluster size (Anikovsky et al., 2008), the fact that the FRET value for the heterodimerization of ErbB2 and ErbB3 is smaller than those for their homoassociations is in agreement with the assumption that ErbB2-3 heteroclusters are smaller than their homoassociations.

We have also observed an increase in the binding of H3.105.5, a conformation-sensitive antibody against ErbB3, upon elisidepsin treatment. The specificity of this increase is underlined by the lack of elisidepsin-induced effect on the binding of other antibodies and the fact that heregulin reverses the increased binding of H3.105.5. We speculate that the membrane effects of elisidepsin might induce a change in the conformation of ErbB3 or in the accessibility of the epitope for H3.105.5. Elisidepsin-induced disruption of large-scale ErbB3 clusters (Landgraf and Eisenberg, 2000), supported by our FRET measurements, may lead to these conformational changes and consequent unmasking of the H3.105.5-binding epitope.

On the other hand, GPI-anchored proteins (GPI–eGFP, PLAP) and ErbB3 were preferentially redistributed upon elisidepsin treatment from the plasma membrane to intracellular vesicles or sometimes even to the nucleus. Although elisidepsin-induced formation of large intracellular vesicles and their progression from the plasma membrane toward the nucleus have been previously reported (Faircloth and Cuevas, 2006), we did not observe the internalization of every kind of membrane protein since ErbB1 and ErbB2 persisted in the plasma membrane after elisidepsin treatment. Although we cannot explain the selectivity profile of elisidepsin in inducing membrane protein internalization, we suspect that elisidepsin-induced membrane effects lead to the specific redistribution of raft-associated membrane proteins including GPI-anchored and ErbB3 proteins (Nagy et al., 2002).

The changes in the fluorescence anisotropy of TMA-DPH and in the generalized polarization of Laurdan immediately after application of the drug preceded cell death and membrane permeabilization reported by propidium iodide uptake by several minutes. All the effects of elisidepsin, including its cytotoxic effect, were very fast. The rapid induction of cell death preceded by changes in the order and fluidity of the plasma membrane are in agreement with the assumption that the primary target of elisidepsin is the plasma membrane and all other effects are the consequences of the primary membrane effects. Fluorescence anisotropy reports the mobility of the fluorescent probe, whereas the generalized polarization of Laurdan is sensitive to the hydration of the plasma membrane (Harris et al., 2002; Parasassi et al., 1991; Sanchez et al., 2007). The combination of decreased fluorescence anisotropy (higher mobility) and increased generalized polarization of Laurdan (lower hydration) is assumed to be characteristic of liquid ordered domains (Harris et al., 2002; Vest et al., 2006) which is followed by detachment of the membrane from the cytoskeleton and membrane permeabilization ("membrane damage"). Elisidepsin-induced increased lipid order has also been reported in a recent publication (Molina-Guijarro et al., 2011).

The elisidepsin-induced changes in the fluorescence anisotropy of TMA-DPH and the generalized polarization of Laurdan in two cell lines (A431 and SKBR-3) having significantly different IC50 values for the drug were identical in direction and similar in magnitude. Elisidepsin was applied at a concentration slightly higher than the IC50 of A431 and significantly larger than that of SKBR-3. In this concentration range effects associated with the mechanism of action of the drug are expected to be manifest. The slightly larger magnitude of changes in anisotropy and generalized polarization in SKBR-3 cells may have been caused by the lower IC50 value of this cell line compared to A431.

Cancer cells display higher sensitivity to Kahalalide F, and presumably to elisidepsin, than their non-tumoral counterparts (Janmaat et al., 2005; Suarez et al., 2003), a finding in apparent disagreement with the

nonspecific membrane effects of elisidepsin. However, cancer cells display characteristic changes in their fatty acid and ganglioside composition. Among others increase in the ratio of saturated/non-saturated fatty acids and accumulation of less-complex gangliosides have been observed (Lopez and Schnaar, 2009; Yin et al., 2006; Yin et al., 2010). In addition, upregulation of fatty acid 2-hydroxylase (FA2H) in malignant tumors has been reported which may lead to the cancer specific cytotoxic effects of elisidepsin (Hama, 2010; Yin et al., 2010). However, tumor hypoxia is known to decrease the rate of hydroxylation due to shortage of oxygen which acts against the tumor-specificity of elisidepsin by reducing the activity of FA2H (Yin et al., 2010). Whether tumor hypoxia could influence the sensitivity of tumor cells to elisidepsin is currently unknown.

In summary, the lack of any correlation between elisidepsin sensitivity and the expression levels of ErbB1–3 questions the role of ErbB proteins in determining elisidepsin responsiveness. Moreover, we also present evidence showing that the preferential changes in the distributions and association states of ErbB and GPI-anchored proteins are secondary to alterations in the cell membrane induced by elisidepsin. Further investigations are required to elucidate how elisidepsin responsiveness is related to structural and dynamic changes of the cell membrane.

Acknowledgments

This work has been supported by research grants from the Hungarian Scientific Research Fund (K72677, K68763), from the European Commission (LSHC-CT-2005-018914, MCRTN-CT-2006-035946-2) and the New Hungary Development Plan co-financed by the European Social Fund and the European Regional Development Fund (TÁMOP-4.2.2-08/1-2008-0019, TÁMOP-4.2.1/B-09/1/KONV-2010-0007).

Appendix A. Supplementary material

Supplementary data to this article can be found online at doi:10.1016/j.ejphar.2011.05.064.

References

Albreht, T., McKee, M., Alexe, D.M., Coleman, M.P., Martin-Moreno, J.M., 2008. Making progress against cancer in Europe in 2008. Eur. J. Cancer 44, 1451–1456.
Anikovsky, M., Dale, L., Ferguson, S., Petersen, N., 2008. Resonance energy transfer in cells: a new look at fixation effect and receptor aggregation on cell membrane. Biophys. J. 95, 1349–1359.
Balogh, G., Horvath, I., Nagy, E., Hoyk, Z., Benko, S., Bensaude, O., Vigh, L., 2005. The hyperfluidization of mammalian cell membranes acts as a signal to initiate the heat shock protein response. FEBS J. 272, 6077–6086.
Brown, D.A., London, E., 1998. Functions of lipid rafts in biological membranes. Annu. Rev. Cell Dev. Biol. 14, 111–136.
Citri, A., Yarden, Y., 2006. EGF-ERBB signalling: towards the systems level. Nat. Rev. Mol. Cell Biol. 7, 505–516.
Di Cosimo, S., Baselga, J., 2008. Targeted therapies in breast cancer: where are we now? Eur. J. Cancer 44, 2781–2790.
Engelke, M., Jessel, R., Wiechmann, A., Diehl, H.A., 1997. Effect of inhalation anaesthetics on the phase behaviour, permeability and order of phosphatidylcholine bilayers. Biophys. Chem. 67, 127–138.
Faircloth, G., Cuevas, C., 2006. Kahalalide F and ES285: potent anticancer agents from marine molluscs. Prog. Mol. Subcell. Biol. 43, 363–379.
Garcia-Rocha, M., Bonay, P., Avila, J., 1996. The antitumoral compound Kahalalide F acts on cell lysosomes. Cancer Lett. 99, 43–50.
Hama, H., 2010. Fatty acid 2-hydroxylation in mammalian sphingolipid biology. Biochim. Biophys. Acta 1801, 405–414.
Harris, F.M., Best, K.B., Bell, J.D., 2002. Use of Laurdan fluorescence intensity and polarization to distinguish between changes in membrane fluidity and phospholipid order. Biochim. Biophys. Acta 1565, 123–128.
Herrero, A.B., Astudillo, A.M., Balboa, M.A., Cuevas, C., Balsinde, J., Moreno, S., 2008. Levels of SCS7/FA2H-mediated fatty acid 2-hydroxylation determine the sensitivity of cells to antitumor PM02734. Cancer Res. 68, 9779–9787.
Holbro, T., Civenni, G., Hynes, N.E., 2003. The ErbB receptors and their role in cancer progression. Exp. Cell Res. 284, 99–110.
Janmaat, M.L., Rodriguez, J.A., Jimeno, J., Kruyt, F.A., Giaccone, G., 2005. Kahalalide F induces necrosis-like cell death that involves depletion of ErbB3 and inhibition of Akt signaling. Mol. Pharmacol. 68, 502–510.
Kenworthy, A.K., Edidin, M., 1998. Distribution of a glycosylphosphatidylinositol-anchored protein at the apical surface of MDCK cells examined at a resolution of <100 A using imaging fluorescence resonance energy transfer. J. Cell Biol. 142, 69–84.
Kuhry, J.G., Fonteneau, P., Duportail, G., Maechling, C., Laustriat, G., 1983. TMA-DPH: a suitable fluorescence polarization probe for specific plasma membrane fluidity studies in intact living cells. Cell Biophys. 5, 129–140.
Kusumi, A., Shirai, Y.M., Koyama-Honda, I., Suzuki, K.G., Fujiwara, T.K., 2010. Hierarchical organization of the plasma membrane: Investigations by single-molecule tracking vs. fluorescence correlation spectroscopy. FEBS Lett. 584, 1814–1823.
Lakowicz, J.R., 2006. Fluorescence Anisotropy. Principles of Fluorescence Spectroscopy. Springer, New York, pp. 353–382.
Landgraf, R., Eisenberg, D., 2000. Heregulin reverses the oligomerization of HER3. Biochemistry 39, 8503–8511.
Lidke, D.S., Nagy, P., Heintzmann, R., Arndt-Jovin, D.J., Post, J.N., Grecco, H.E., Jares-Erijman, E.A., Jovin, T.M., 2004. Quantum dot ligands provide new insights into erbB/HER receptor-mediated signal transduction. Nat. Biotechnol. 22, 198–203.
Ling, Y.H., Aracil, M., Jimeno, J., Perez-Soler, R., Zou, Y., 2009. Molecular pharmacodynamics of PM02734 (elisidepsin) as single agent and in combination with erlotinib; synergistic activity in human non-small cell lung cancer cell lines and xenograft models. Eur. J. Cancer 45, 1855–1864.
Lopez, P.H., Schnaar, R.L., 2009. Gangliosides in cell recognition and membrane protein regulation. Curr. Opin. Struct. Biol. 19, 549–557.
Martin-Algarra, S., Espinosa, E., Rubio, J., Lopez Lopez, J.J., Manzano, J.L., Carrion, L.A., Plazaola, A., Tanovic, A., Paz-Ares, L., 2009. Phase II study of weekly Kahalalide F in patients with advanced malignant melanoma. Eur. J. Cancer 45, 732–735.
Matkó, J., Nagy, P., 1997. Fluorescent lipid probes 12-AS and TMA-DPH report on selective, purinergically induced fluidity changes in plasma membranes of lymphoid cells. J. Photochem. Photobiol. B 40, 120–125.
Molina-Guijarro, J.M., Moneo, V., Martinez-Leal, J.F., Cuevas, C., Garcia-Fernández, L.F., Galmarini, C.M., 2009. PM02734, a new marine-derived antitumoral compound, has rapid effects on membrane integrity and permeability in tumor cells. Abstract 888. 100th Annual Meeting of the American Association for Cancer Research, Denver, CO.
Molina-Guijarro, J.M., Macías, Á., García, C., Muñoz, E., García-Fernández, L.F., David, M., Núñez, L., Martínez-Leal, J.F., Moneo, V., Cuevas, C., Lillo, M.P., Villalobos Jorge, C., Valenzuela, C., Galmarini, C.M., 2011. Irvalec inserts into the plasma membrane causing rapid loss of integrity and necrotic cell death in tumor cells. PLoS One 6, e19042.
Nagy, P., Jenei, A., Kirsch, A.K., Szöllősi, J., Damjanovich, S., Jovin, T.M., 1999. Activation-dependent clustering of the erbB2 receptor tyrosine kinase detected by scanning near-field optical microscopy. J. Cell Sci. 112, 1733–1741.
Nagy, P., Vereb, G., Sebestyén, Z., Horváth, G., Lockett, S.J., Damjanovich, S., Park, J.W., Jovin, T.M., Szöllősi, J., 2002. Lipid rafts and the local density of ErbB proteins influence the biological role of homo- and heteroassociations of ErbB2. J. Cell Sci. 115, 4251–4262.
Nagy, P., Vereb, G., Damjanovich, S., Mátyus, L., Szöllősi, J., 2006. Measuring FRET in flow cytometry and microscopy. In: Robinson, J.P. (Ed.), Current Protocols in Cytometry. John Wiley & Sons, pp. 12.18.11–12.18.13.
Parasassi, T., De Stasio, G., Ravagnan, G., Rusch, R.M., Gratton, E., 1991. Quantitation of lipid phases in phospholipid vesicles by the generalized polarization of Laurdan fluorescence. Biophys. J. 60, 179–189.
Provencio, M., Sanchez, A., Gasent, J., Gomez, P., Rosell, R., 2009. Cancer treatments: can we find treasures at the bottom of the sea? Clin. Lung Cancer 10, 295–300.
Sanchez, S.A., Tricerri, M.A., Gunther, G., Gratton, G., 2007. Laurdan Generalized polarization: from cuvette to microscope. In: Méndez-Vilas, A., Díaz, J. (Eds.), Modern Research and Educational Topics in Microscopy. Applications in Biology and Medicine. Formatex, pp. 1007–1014.
Sear, J.W., 2009. What makes a molecule an anaesthetic? Studies on the mechanisms of anaesthesia using a physicochemical approach. Br. J. Anaesth. 103, 50–60.
Sharma, P., Varma, R., Sarasij, R.C., Ira, Gousset, K., Krishnamoorthy, G., Rao, M., Mayor, S., 2004. Nanoscale organization of multiple GPI-anchored proteins in living cell membranes. Cell 116, 577–589.
Suarez, Y., Gonzalez, L., Cuadrado, A., Berciano, M., Lafarga, M., Munoz, A., 2003. Kahalalide F, a new marine-derived compound, induces oncosis in human prostate and breast cancer cells. Mol. Cancer Ther. 2, 863–872.
Szabó, A., Horváth, G., Szöllősi, J., Nagy, P., 2008. Quantitative characterization of the large-scale association of ErbB1 and ErbB2 by flow cytometric homo-FRET measurements. Biophys. J. 95, 2086–2096.
Szentesi, G., Horváth, G., Bori, I., Vámosi, G., Szöllősi, J., Gáspár, R., Damjanovich, S., Jenei, A., Mátyus, L., 2004. Computer program for determining fluorescence resonance energy transfer efficiency from flow cytometric data on a cell-by-cell basis. Comput. Methods Programs Biomed. 75, 201–211.
Tzahar, E., Waterman, H., Chen, X., Levkowitz, G., Karunagaran, D., Lavi, S., Ratzkin, B.J., Yarden, Y., 1996. A hierarchical network of interreceptor interactions determines signal transduction by Neu differentiation factor/neuregulin and epidermal growth factor. Mol. Cell. Biol. 16, 5276–5287.
Vest, R., Wallis, R., Jensen, L.B., Haws, A.C., Callister, J., Brimhall, B., Judd, A.M., Bell, J.D., 2006. Use of steady-state laurdan fluorescence to detect changes in liquid ordered phases in human erythrocyte membranes. J. Membr. Biol. 211, 15–25.
Yin, J., Hashimoto, A., Izawa, M., Miyazaki, K., Chen, G.Y., Takematsu, H., Kozutsumi, Y., Suzuki, A., Furuhata, K., Cheng, F.L., Lin, C.H., Sato, C., Kitajima, K., Kannagi, R., 2006. Hypoxic culture induces expression of sialin, a sialic acid transporter, and cancer-associated gangliosides containing non-human sialic acid on human cancer cells. Cancer Res. 66, 2937–2945.
Yin, J., Miyazaki, K., Shaner, R.L., Merrill Jr., A.H., Kannagi, R., 2010. Altered sphingolipid metabolism induced by tumor hypoxia — new vistas in glycolipid tumor markers. FEBS Lett. 584, 1872–1878.
Zurita, A.R., Crespo, P.M., Koritschoner, N.P., Daniotti, J.L., 2004. Membrane distribution of epidermal growth factor receptors in cells expressing different gangliosides. Eur. J. Biochem. 271, 2428–2437.

Supplementary material

Table S1 ErbB expression profile of the cell lines used

Cell line	Number of proteins/cell ($\times 10^3$)		
	ErbB1	ErbB2	ErbB3
CHO	0	~0	0
CHO-ErbB2	0	200	0
CHO-ErbB2-3	0	200	100
A431	2000	20	3
A4erbB1	3100	20	1.5
A4erbB2	1200	950	1.5
A4erbB3	2000	20	800
SKBR-3	50	800	15

The expression level of ErbB proteins was determined by flow cytometry using Qifikit (Dako, Glostrup, Denmark). The numbers represent the mean of three independent experiments.

Fig. S1 Fluorescence microscopic investigation of the short-term effect of elisidepsin on parental and transfected A431 cells

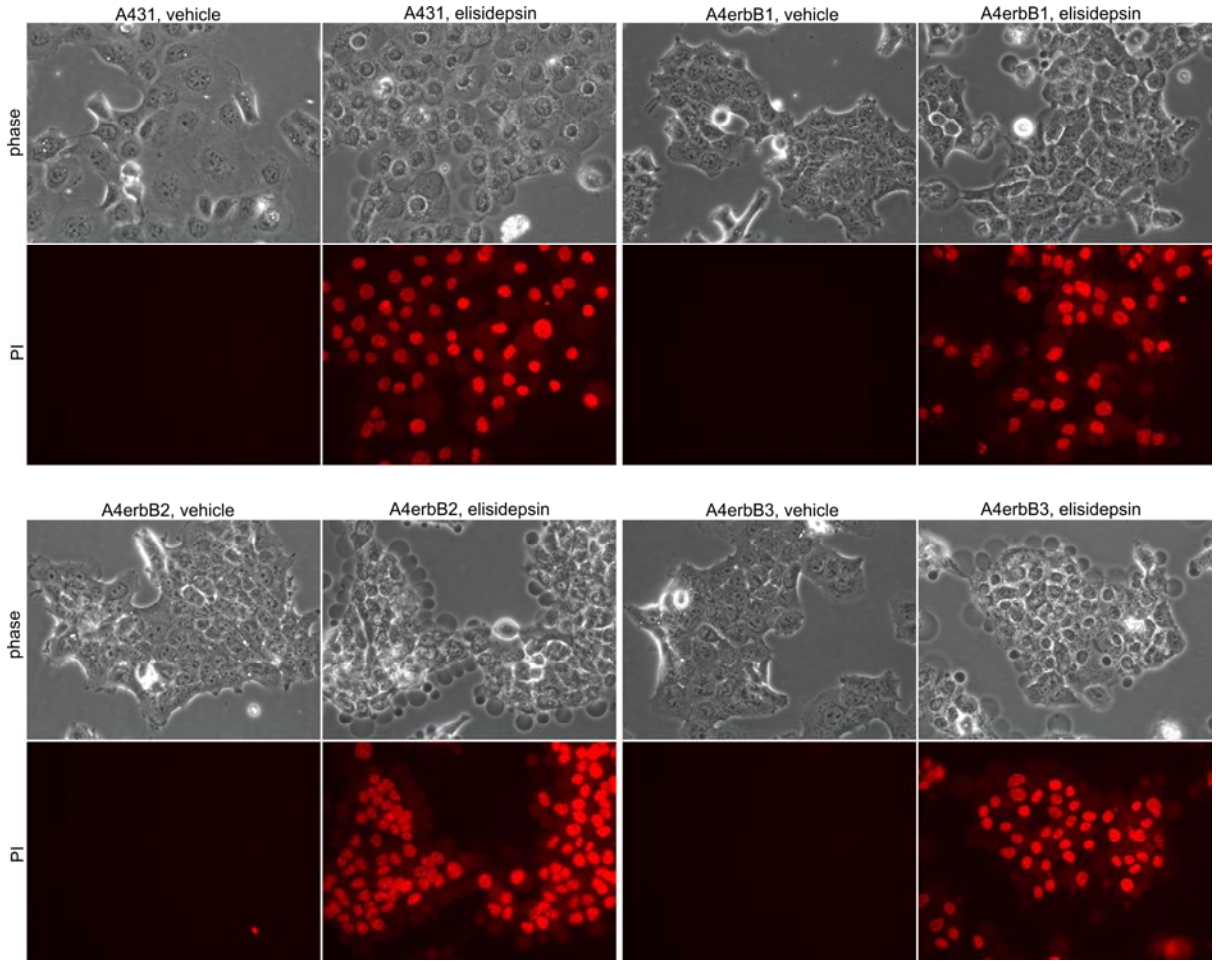

Untransfected, ErbB1-eGFP- (A4erbB1), ErbB2-mYFP- (A4erbB2) and ErbB3-citrine-transfected (A4erbB3) A431 cells were treated with elisidepsin or vehicle in the presence of propidium iodide for 30 min followed by acquiring fluorescence and phase contrast images.

Fig. S2 RNA interference-mediated knock-down of ErbB3 expression

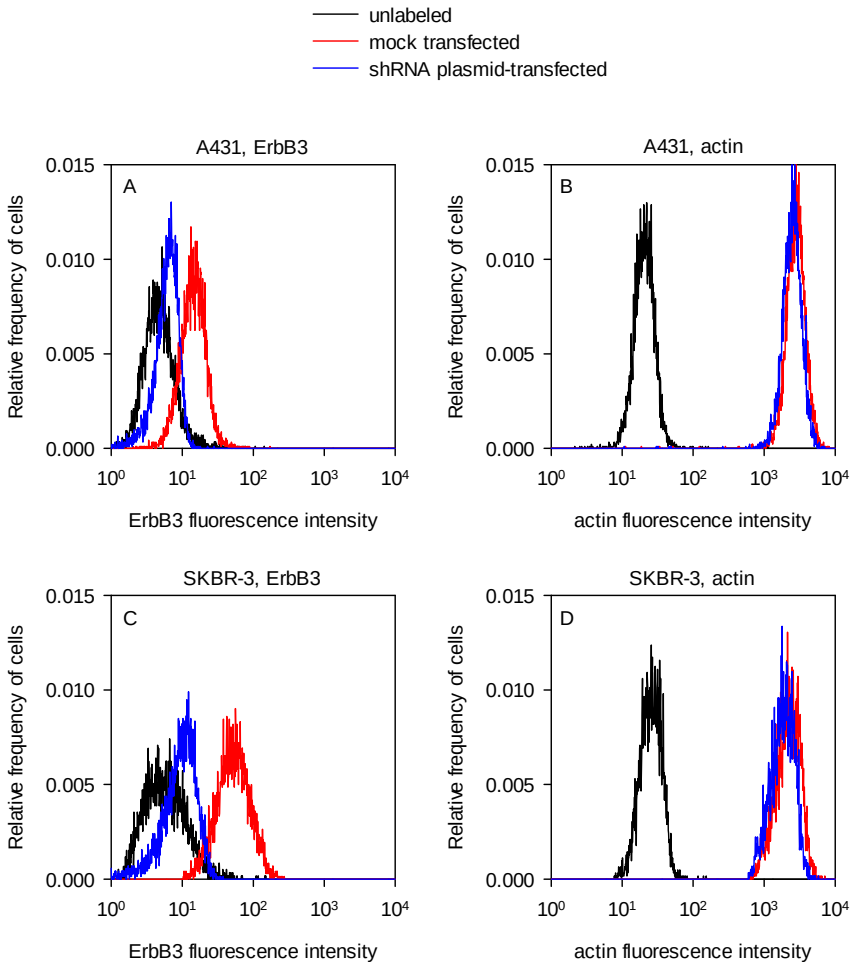

A431 and SKBR-3 cells were transfected by electroporation with a plasmid producing a shRNA against ErbB3. 60 hours after transfection cells were harvested, fixed, permeabilized and stained for ErbB3 (panels A,C) using a primary fluorescently labeled antibody against ErbB3 (H3.90.6). In order to show the lack of any significant effect of transfection and shRNA production on the expression of an irrelevant gene fixed and permeabilized cells were labeled with a monoclonal antibody against actin (clone AC40, Sigma-Aldrich) followed by secondary staining with an AlexaFluor647-labeled anti-mouse antibody (panels B,D).